Microphase Separation in a Model Graft Copolymer

W. D. Dozier and P. Thiyagarajan
Intense Pulsed Neutron Source
Argonne National Laboratory
Argonne, IL 60439

D. G. Peiffer, M. Rabeony, S. K. Behal, M. M. Disko
Exxon Research & Engineering Co.
Annandale, NJ 08801

M. Y. Lin
Reactor Radiation Division
NIST
Gaithersburg, MD 20899

October, 1993

DISCLAIMER

/sm

Polymers, laminations & coatings Boston MA 9/7-10/93

To be submitted to the Proceedings of the 6th International Symposium and to be published by the Journal of Applied Polymer Science.
This work is supported by the U.S. Department of Energy, Basic Energy Sciences, Materials Sciences Contract #W31-109-ENG-38.

Microphase Separation in a Model Graft Copolymer

W. D. Dozier,[a] D. G. Peiffer,[b] M. Y. Lin,[c] M. Rabeony,[b] P. Thiyagarajan,[a] S. K. Behal[b] & M. M. Disko[b]

[a]*Intense Pulsed Neutron Source*
Argonne National Laboratory
Argonne, IL 60439

[b]*Exxon Research & Engineering Co.*
Rt. 22 East
Clinton Township
Annandale, NJ 08801

[c] *Reactor Radiation Division*
NIST
Route 117 and Quince Orchard Rd.
Gaithersburg, MD 20899

Abstract We present a preliminary overview of our work on a series of graft copolymers having poly(ethyl acrylate) backbones with pendant chains of polystyrene (PS). The copolymer system appeared to be in the strong segregation limit and exhibited evidence of ordered structures. The morphology of these structures can apparently be very different from what would be expected. For instance, we observed a lamellar structure in a material containing 28 wt. % PS grafts. Samples under uniaxial strain showed either conventional (i.e., affine deformation) and anomalous ("butterfly" isointensity patterns) behavior in small-angle neutron scattering.

Introduction

Since the entropy of mixing of polymers is typically very small, any repulsive interaction will result in blends that are, over some temperature range, unstable with respect to phase separation. Therefore, the production of useful polymer blends typically requires the use of compatibilizers, which enhance mixing by limiting the size of domains that result from the phase separation of incompatible homopolymers. It is well established that compatibilizers enhance blend properties.[1] These materials are usually graft or block copolymers in which chain segments interact and "bridge" the interfacial boundary of the phase separated regions. Compatibilization is often effected by the formation of graft copolymers *in situ* under reactive processing conditions.[2, 3]

The understanding of the phase behavior of diblock copolymers has progressed considerably in recent years.[4] While diblocks are important both in their own right and as tractable model materials, the study of other, more complex copolymer architectures is also important. First, it will be significant to know under what conditions they behave differently from diblocks. This will help define the applicability of the extensive diblock copolymer literature to particular applications. Also, it is reasonable to expect that graft copolymers and other more complex copolymer structures will exhibit quite different behavior that will have relevance to applications.

Our graft copolymers consisted of poly(ethyl acrylate) (PEA) backbones onto which polystyrene (PS) grafts were attached at random sites. They are called "model" materials because their structures are expected to be somewhat better-defined than *in situ* compatibilizers. Preliminary results are presented here from

small-angle neutron scattering (SANS), neutron reflection (NR) and transmission electron microscopy (TEM).

Experimental

Synthesis

The PEA-g-PS materials were synthesized by a macromonomer technique.[5] Monodisperse PS chains, having a M_n of 14.6 kg/mole and a methacrylate endgroup, were added to partially deuterated ethyl acrylate monomer[6] and polymerized via free radical polymerization. The PS chains then were included at random as grafts onto the PEA backbone. Each of the resulting graft copolymer materials had a total number-averaged molecular weight (M_n) of ≈ 150 kg/mole. Three compositions were prepared, having 9, 28 and 48 wt.% PS grafts, corresponding to an average of 1, 3 and 5 PS grafts per molecule, respectively.

SANS

Thick (≈ 0.5 mm) films were prepared for SANS by melt pressing.[6] The samples were annealed in the press for 6 hours at 130°C. Squares (2.5 cm x 2.5 cm) were cut from the films and in a stretching device that allowed for the application of a uniaxial strain. The stretching device could then reach a maximum elongation ratio (λ) of about 3. We applied strain to the samples in steps, never allowing it to relax until the measurements were complete, a time period on the order of one day. Of course, since the PEA component is elastomeric, there would be some relaxation of stress in the material. Upon releasing the clamps after the measurements were completed, the samples would typically not return very much towards their original length. We were able to

stretch the 9 wt.% material to the limit of the device, but the 28 wt.% would usually break before reaching $\lambda = 2$, and the 48 wt.% PS material could not be stretched in this manner at all. SANS measurements were performed on the NG7 instrument at the National Institute of Standards and Technology and SAD at Argonne's Intense Pulsed Neutron Source (IPNS).

NR

We prepared thin (1000 - 2000 Å) film samples for NR study by spin-coating from toluene solution onto silicon substrates. The substrates were prepared beforehand by soaking in chromic sulfuric acid, rinsing in deionized water and rinsing with toluene. The film thicknesses were determined by ellipsometry.

The samples were then annealed in a vacuum oven (≈ 1 mT) for 24 hours at 130°C. Neutron reflection data were obtained on POSY-II at IPNS.[7] Neutron reflection is an effective means to determine the chemical depth profile in systems that have been labeled for neutron contrast. The details of the NR technique have been considered elsewhere.[8]

The reflectivity $R(k)$, where k is the momentum transfer normal to the sample plane,

$$k = \frac{2\pi}{\lambda}\sin\theta, \qquad (1)$$

(where θ is the angle of incidence/reflection) is a phaseless, non-linear transform of the depth profile. No inverse transform has been developed, even with the phase, so the typical procedure is to fit the parameters of a model profile to the data via χ^2 minimization.

Results & Discussion

SANS

Unstretched samples

The SANS spectra from each of the three samples are shown in Figure 1. There is a single scattering peak in each spectrum. In order to characterize this peak, we fit the data with the following expression:

$$S(q) \propto \frac{1/q^{\alpha}}{1+(q-q_0)^2\xi^2}, \tag{2}$$

where q is the scattering vector, given by:

$$q = \left(4\pi/\lambda\right)\sin\left(\theta/2\right), \tag{3}$$

where λ is the neutron wavelength and θ is the scattering angle. This functional form was chosen because it fit the data reasonably well in the vicinity of the peak. From the position of the peak, we can determine an average domain spacing L and from the "correlation length" ξ we can get a measure of the strength of the ordering in the sample. The resulting parameters are shown in Table 1. The average domain spacing decreases with grafting level as would be expected. Note that also ξ decreases as the number of grafts increases; we will return to this point below.

Note that in Figure 1 and in all later figures containing SANS data, we have subtracted an estimated constant background due to incoherent scattering from protons. The high level of incoherent scattering make determination of the Porod exponent from these data impossible.

Stretched samples

The 2-dimensional SANS spectra for the stretched 9 wt.% sample are shown in Figure 2. Let us call the stretching direction the x axis and the direction normal to the strain the y axis. The pattern in Figure 2 is the usual "two-point" elliptical one seen in strained rubbers. Rather than integrating the full circle as is typically done in SANS, we integrated the data in wedges that were ±30° from either the x or y axis. The resulting curves are shown in Figure 3. These curves can in turn be fitted by Equation 2 and the resulting positions and widths of the scattering peaks as a function of the elongation ratio for the 9 wt.% PS sample are shown in Figure 4.

The position of the peak in the x direction is essentially a linear function of the elongation ratio λ, while that in the y direction appears to be independent of λ. This is characteristic of a quasi-affine deformation. Since one would expect that the morphology of this sample is some quasi-periodic arrangement of spheres or cylinders (due to the small amount of PS), this behavior is not surprising.

Two-dimensional contour plots of the SANS from a 28 wt.% PS sample are shown in Figure 5. Note the appearance of the "abnormal butterfly" patterns that appear at the lowest λ.[9-12] Similar patterns have been observed in these samples via light scattering, indicating that its origin is at long (≈ 100 - 1000 nm) length scales. Looking at the higher-q regions of the contour plots and at the IPNS data which does not include much of the data in the low-q region below the peak, we can see the scattering pattern change over to one that is more like the conventional elliptical pattern.[13] In fact, applying a function like Equation 2 to these (higher-q) data result in anisotropy in L, but not in ξ. In butterfly patterns arising from gels, the "correlation length" is typically quite anisotropic.[12] All of

this probably means that the butterfly phenomenon is more connected to the response of the regions over which the lamellae have a correlated orientation. This length scale appears to be on the order of 1000 Å.

Neutron Reflection

Specular neutron reflectivities are plotted for the three materials in Figure 7, along with the model profiles used to produce the fitted curves. We fit the data with model profiles of the following form:[14, 15]

$$\phi(z) = \phi_0 + \left(e^{-z/\xi} + e^{(z-z_0)/\xi}\right)\sum_i \left[a_i \cos\left(\frac{2\pi z}{L}\right) + b_i \sin\left(\frac{2\pi z}{L}\right)\right], \qquad (4)$$

where L is the spatial period of the structure, z is the distance from the substrate surface, z_0 is the total film thickness and ξ is the characteristic distance over which the ordering (or orientation) persists away from the interfaces. This model assumes that the orientation or ordering is induced and/or pinned at the interfaces and that the spatial period is constant throughout the sample. Model-free treatment of the data via a Maximum Entropy technique[16] produced similar profiles. The more important of the fitted parameters are listed in Table 2.

The profile from the 9 wt.% PS sample shows a periodic structure that propagates throughout the film. Note that the maximum PS volume fraction is about 30%. This fits well with the hypothesis that this sample has a morphology consisting of an ordered array of spheres or cylinders.

The NR data from the 28 wt.% PS thin films can only be successfully modeled with a lamellar profile, with alternating layers of 100% PEA and nearly 100% PS. This is a surprising result. Given the architecture of the graft copolymers, one expects the PEA-PS interface to bend strongly toward the (PS) graft component,

even for compositions > 50% PS. In fact, one can estimate what composition will give rise to a flat interface by using a modified form of a criterion for flat interfaces in diblock copolymer melts:[17]

$$\phi_{PS}^2 a_{PS} \sigma_{PS}^3 = \phi_{PEA}^2 a_{PEA} \sigma_{PEA}^3. \qquad (5)$$

where σ is the areal density of chains, ϕ is the volume fraction of a given species and a is the "packing length," a measure of the flexibility of the chain (given by: $a = 3m_0/C_\infty b^2 \rho$, where m_0 is the volume per backbone bond, b is the bond length and C_∞ is the characteristic ratio). For diblocks, $\sigma_A = \sigma_B = \sigma$, but for graft copolymers there are two backbone chains for each graft chain at the interface, so $\sigma_{PEA} = 2\sigma_{PS} = 2\sigma$. Inserting literature values for the a's leads to the conclusion that a flat interface will result with a composition of 72% PS.

The appearance of a lamellar structure was surprising enough that, even though the scattering data were compelling, we sought corroboration from real-space probes. Figure 8 is a transmission electron micrograph of a 28 wt.% PS sample in which the PS has been stained with ruthenium tetroxide. Note the "fingerprint"-like appearance that is characteristic of lamellar microstructures. Tilting the samples showed no indication of cylinders and in fact, the sample is so polycrystalline that one would expect that if the morphology were cylindrical there would be some indication of this at any tilt angle.

We have two principal hypotheses as to the origin of this lamellar phase. First, it is well established that polydispersity will reduce the elastic energy in a polymer melt.[18] Therefore, we expect that the polydispersity of the backbone molecular weight will lead to less than expected elastic energy and hence less

than expected curvature of the interface towards the graft component. This effect is in the right direction, but it is not yet known if it has the correct magnitude.

The other, and probably more important, possible cause for this result is the randomness of the graft placements. There are, no doubt, many attachments where the molecular weight between grafts is very small. This situation will lead to more phase mixing on the PS side of the PS-PEA interface. This is probably what is seen in modeling the NR data. Note that the model profile has layers of 100% PEA, but that the PS layers never quite reach the pure PS level, and that the mixing is more pronounced at the boundaries. Also, the alternating layers are nearly equal in thickness. This appears to be the case in the TEM photo, as well, and if it were not so, it would be reflected in the second order Bragg peaks in Equation 4 and therefore easily visible in the NR data. All of these characteristics are consistent with the randomness of graft placement causing phase mixing at or near the interface.

Conclusions

We have characterized a family of PEA-g-PS model graft copolymer compatibilizers via SANS and NR. In doing so, we have found that these copolymers are strongly phase separated into quasiperiodic structures. One of these materials produced the unexpected results of abnormal butterfly patterns in SANS spectra and a lamellar morphology in spite of its highly asymmetric composition and architecture. Further work is planned and/or underway on these materials: SAXS, to determine the high-q (Porod) exponent that will give some additional information as to the structure of the PEA-PS interface in the neat copolymer, SANS on homopolymer blends to test directly the compatibilization as a function of grafting level and NR on

homopolymer/copolymer/homopolymer "sandwiches" which will inform about the structure of the interface in blends.

Acknowledgments

The technical assistance of P. Wright, M. Olveria, R. Goyette and D. Wozniak and helpful discussions with M. Olvera de la Cruz, T. Witten, A. Karim and N. Singh are gratefully acknowledged. The neutron reflection data was collected with the assistance of G. Agrawal. Work at Argonne is supported by US DOE, BES-MS contract #W-31-109-ENG-38.

References

1. Utracki, L. A., Walsh, D. J. & Weiss, R. A. *Polymer Alloys, Blends and Ionomers* (American Chemical Society, Washington, D.C., 1989).

2. Lambla, M. & Seadan, M. *Polym Eng Sci* **32,** 1687 (1992).

3. Xanthos, M. & Dagli, S. S. *Polym Eng Sci* **31,** 929 (1991).

4. Bates, F. S. *Science* **251,** 898 (1991).

5. Rabeony, M., Peiffer, D. G., Dozier, W. D. & Lin, M. Y. *Macrom* **26,** 3676 (1993).

6. Dozier, W. D., Peiffer, D. G., Lin, M. Y., Rabeony, M., Thiyagarajan, P., Agrawal, G. & Wool, R. P. *Polymer Communications* submitted for publication.

7. Karim, A., Arendt, B. H., Goyette, R., Huang, Y. Y., Kleb, R. & Felcher, G. P. *Phys B* 173, 17-24 (1991).

8. Russell, T. P. *Mat Sci Rep* 5, 171 (1990).

9. Oeser, R., Picot, C. & Herz, J. *Spring Proc Phys* 29, 104 (1987).

10. Oeser, R. (Ph. D. thesis, Johannes Gutenberg Universität, Mainz), 1992.

11. Bastide, J., Boué, F. & Buzier, M. *Spring Proc Phys* **29**, 112 (1987).

12. Bastide, J., Leibler, L. & Prost, J. *Macrom* **23**, 1821 (1990).

13. Boue', F., Bastide, J., Buzier, M., Lapp, A., Herz, J. & Vilgis, T. A. *Colloid & Polymer Science* **269**, 195 (1991).

14. Singh, N., Tirrell, M. & Bates, F. S., preprint.

15. Foster, M. D., Sikka, M., Singh, N., Bates, F. S., Satija, S. K. & Majkrazk, C. F. *J Chem Phys* **96**, 8605 (1992).

16. Sivia, D. S., Hamilton, W. A. & Smith, G. S. *Phys B* **173**, 121 (1991).

17. Witten, T. A., Milner, S. T. & Wang, Z.-G. in *Multiphase Macromolecular Systems* (ed. Culbertson, B.M.) (Plenum, New York, 1989).

18. Graessley, W. W. *Adv Polym Sci* **16**, 1 (1974).

Tables

ϕ_{PS}	q_0, Å^{-1}	$L \approx \frac{2\pi}{q_0}$, Å	ξ, Å
0.09	0.0190	330	200
0.28	0.0213	295	155
0.48	0.0255	245	140

Table 1. Results from SANS ϕ_{PS} is the weight fraction of PS grafts, the other quantities are as defined in Equation 2.

ϕ_{PS}	L, Å	ξ, Å	L_{NR}/L_{SANS}
0.09	295	540	0.89
0.28	243	∞	0.82
0.48	220	180	0.90

Table 2. Results from NR ϕ_{PS} is the weight fraction of PS grafts, the other parameters are as defined in Equation 4.

Figure Captions

Figure 1. SANS spectra from each of the three materials studied. a) 9 wt. % PS grafts, b) 28 wt. % PS grafts and c) 48 wt. % PS grafts. The open symbols are NIST data and the solid symbols are IPNS data.

Figure 2. Two-dimensional contour plots of SANS spectra from 9 wt. % sample undergoing uniaxial strain. The stretching direction is vertical in all plots, with the range of q in each the same as that of the NIST data in Figure 1. The elongation ratios are, counter-clockwise from top left, 1.00, 1.50, 2.00, 3.00.

Figure 3. Wedge-averaged intensity data from 9 wt. % PS sample, in directions a) parallel to, and b) perpendicular to the stretching direction. The circles, squares, diamonds, x's and crosses correspond to elongation ratios (λ) of 1.00 ,1.20 , 1.50, 2.00 and 3.00, respectively.

Figure 4. The a) position and b) width of the scattering peaks in the data from Fgiure 3 (circles: parallel to stretch, squares, perpendicular to stretch) as a function of λ.

Figure 5. Two-dimensional contour plots of SANS spectra from 28 wt. % sample undergoing uniaxial strain. Again, the stretching direction is vertical in all plots, and the range of q in each is the same as that of the NIST data in Figure 1. The elongation ratios are, counter-clockwise from top left, 1.00, 1.08, 1.28, 2.35.

Figure 6. Wedge-averaged intensity data from 28 wt. % PS sample, in directions a) parallel to, and b) perpendicular to the stretching direction. The circles, squares, diamonds and x's correspond to elongation ratios (λ) of 1.00, 1.08, 1.28 and 2.35, respectively.

Figure 7. Specular neutron reflectivities and fitted model profiles for each of the three materials, annealed 24 hours at 130° C: a) & b) 9 wt. % PS, c) & d) 28 wt. % PS and e) & f) 48 wt. % PS. Solid lines are generated from the model profiles which resulted from adjusting the parameters in the model described by Equation 4.

Figure 8. Transmission electron micrograph of 28 wt. % PS sample stained with ruthenium tetroxide.

Figures

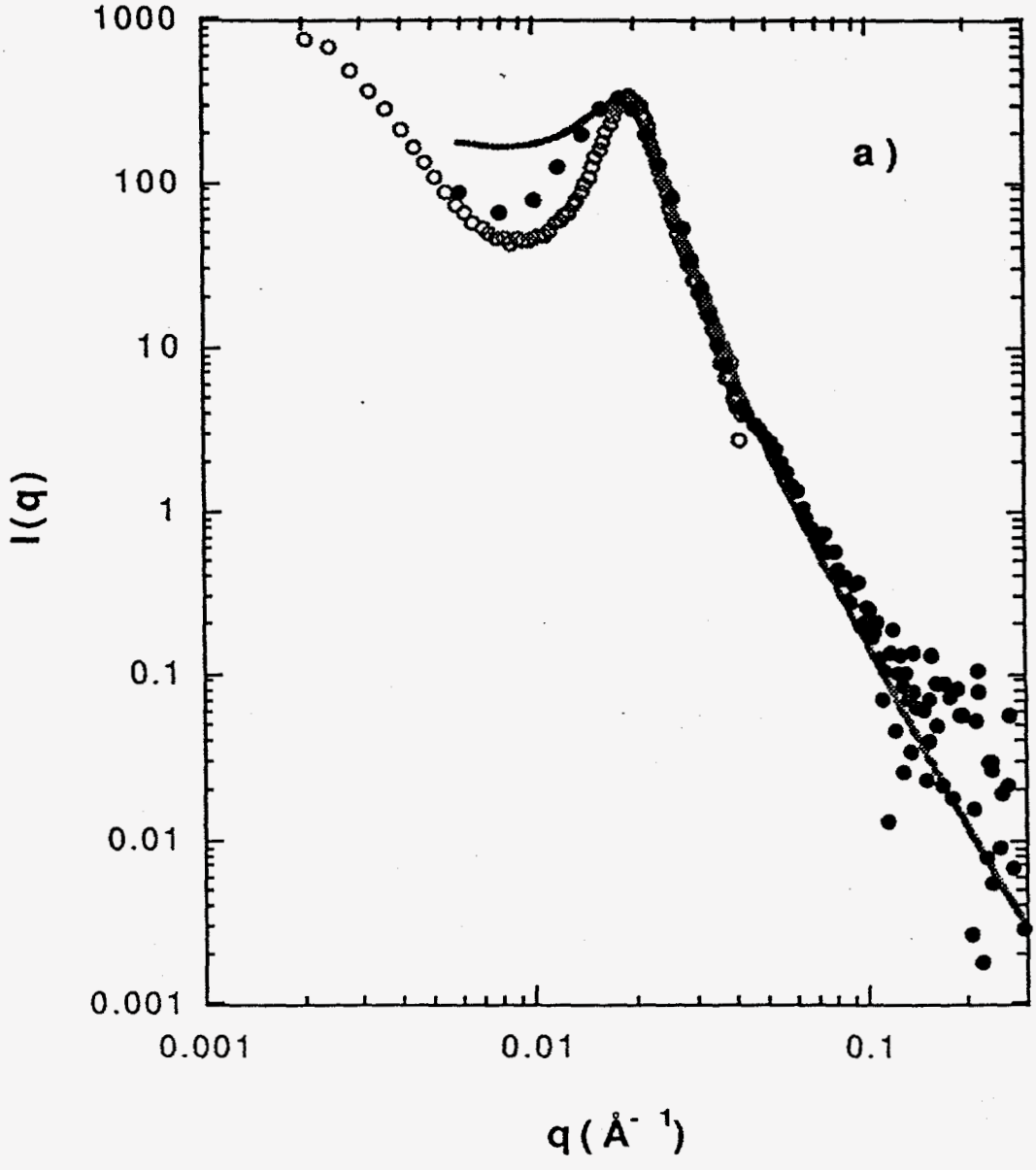

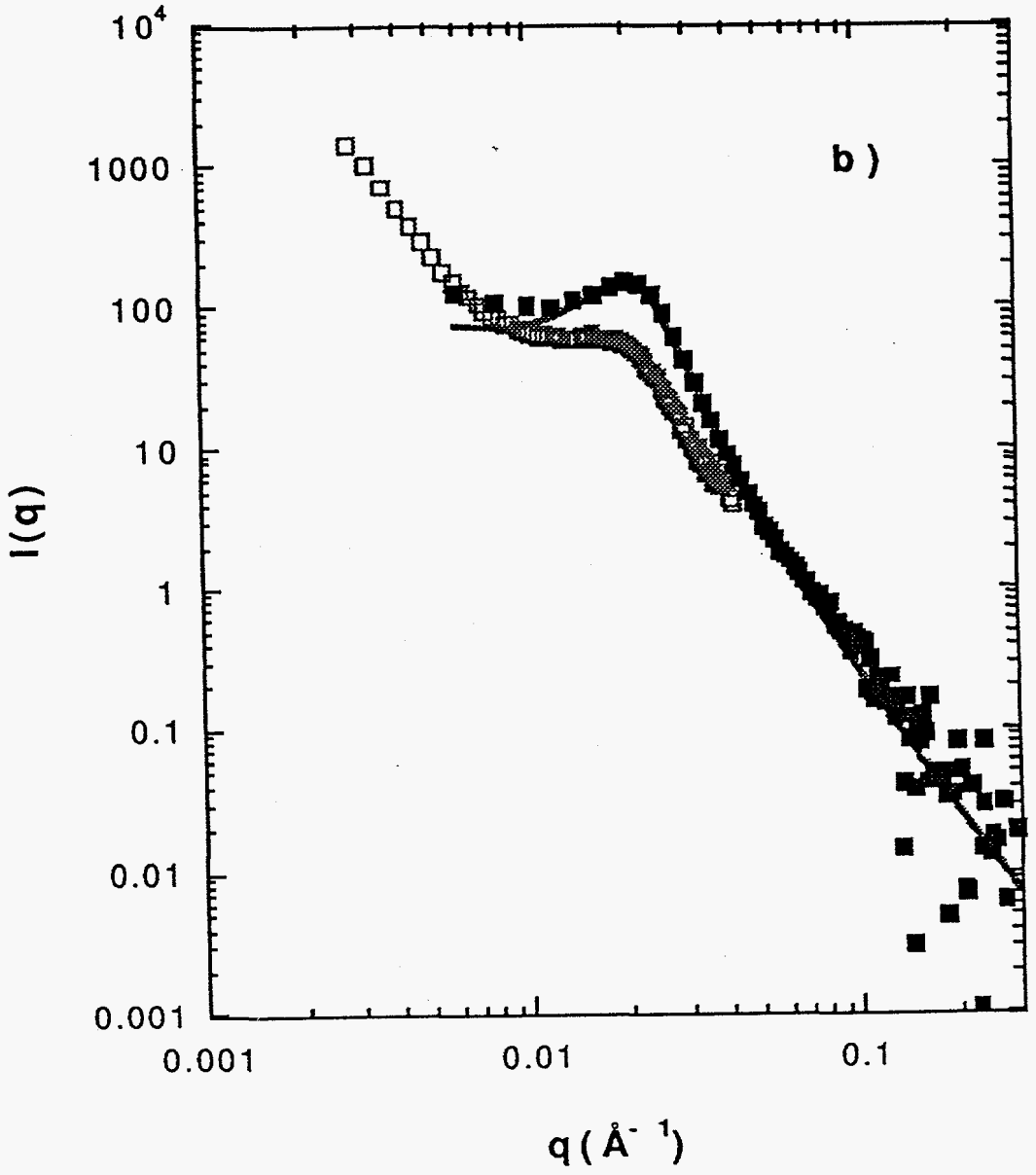
b)
I(q)
q (Å⁻ ¹)
10⁴
1000
100
10
1
0.1
0.01
0.001
0.001
0.01
0.1

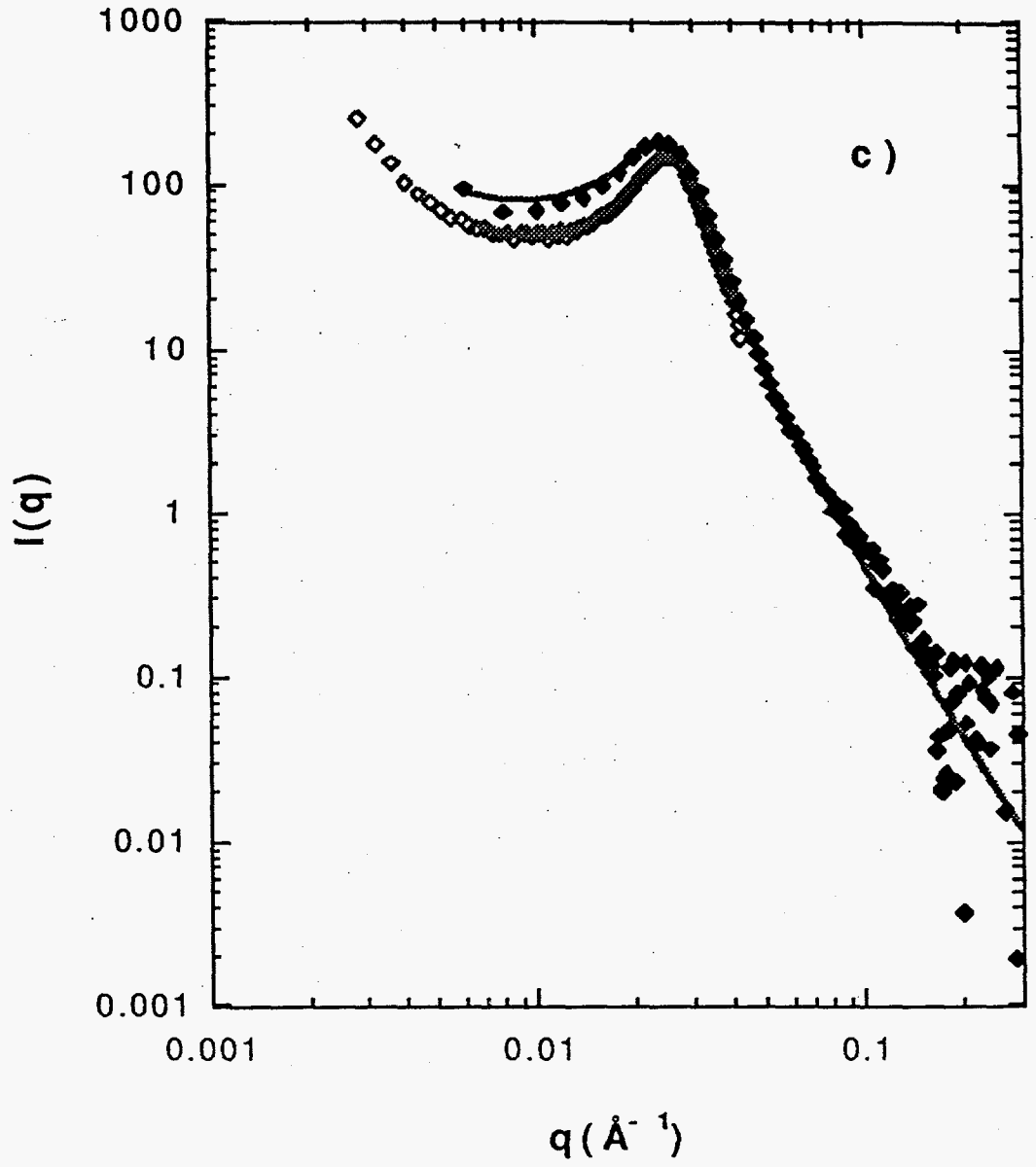
1000
100
10
1
0.1
0.01
0.001
I(q)
c)
0.001
0.01
0.1
q (Å⁻ ¹)

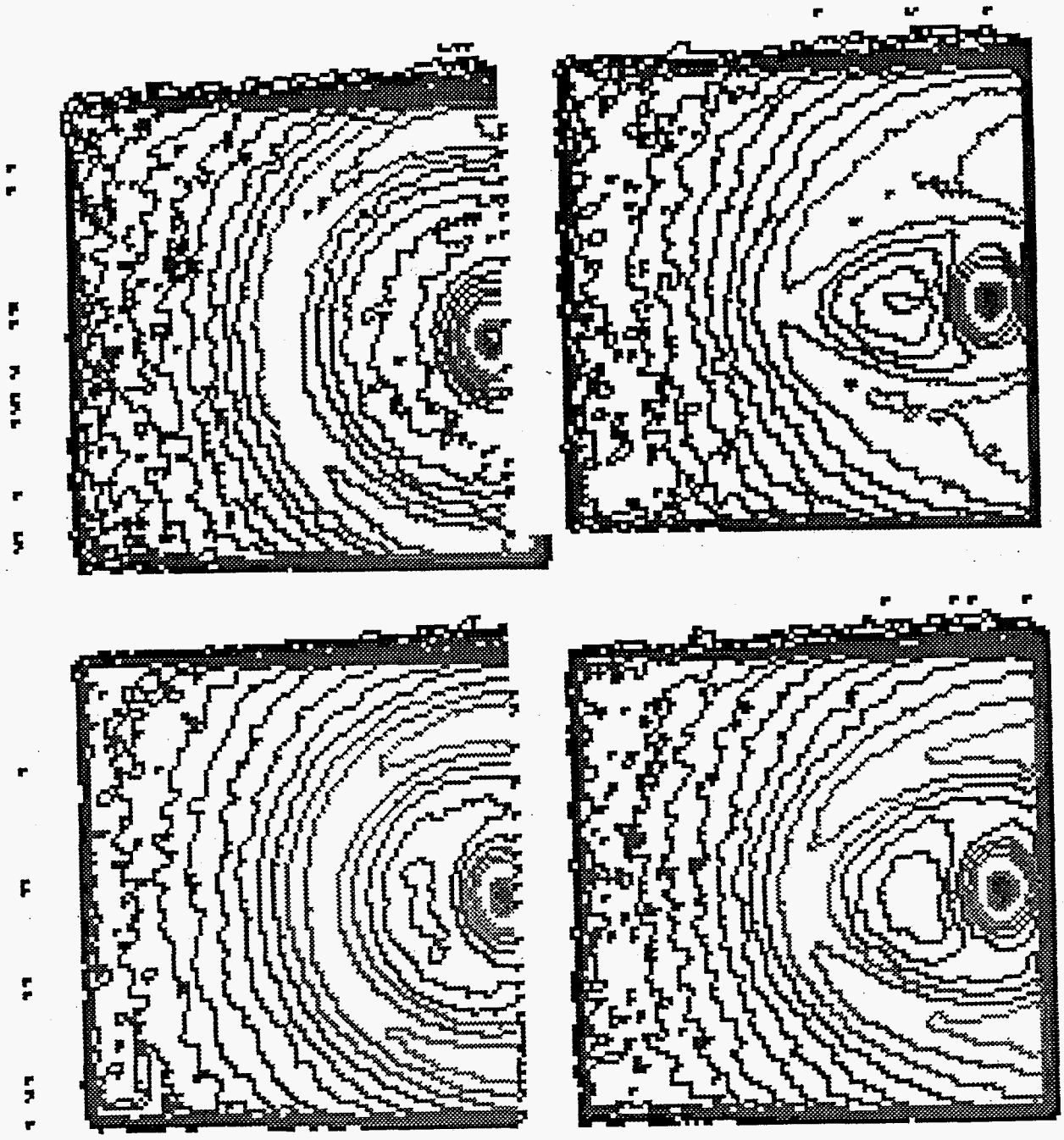

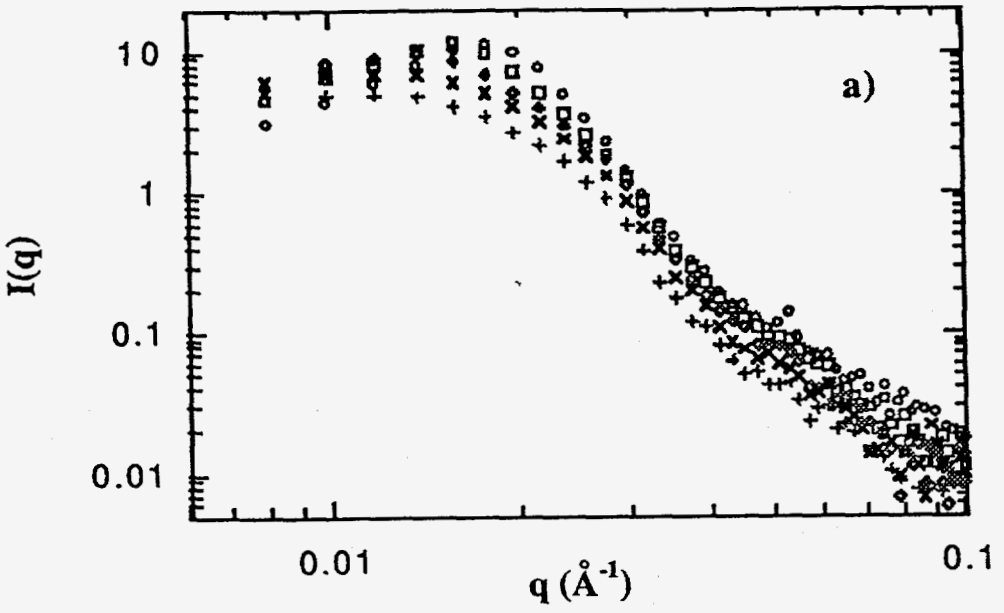
a)
10
1
0.1
0.01
I(q)
0.01
0.1
q (Å-1)

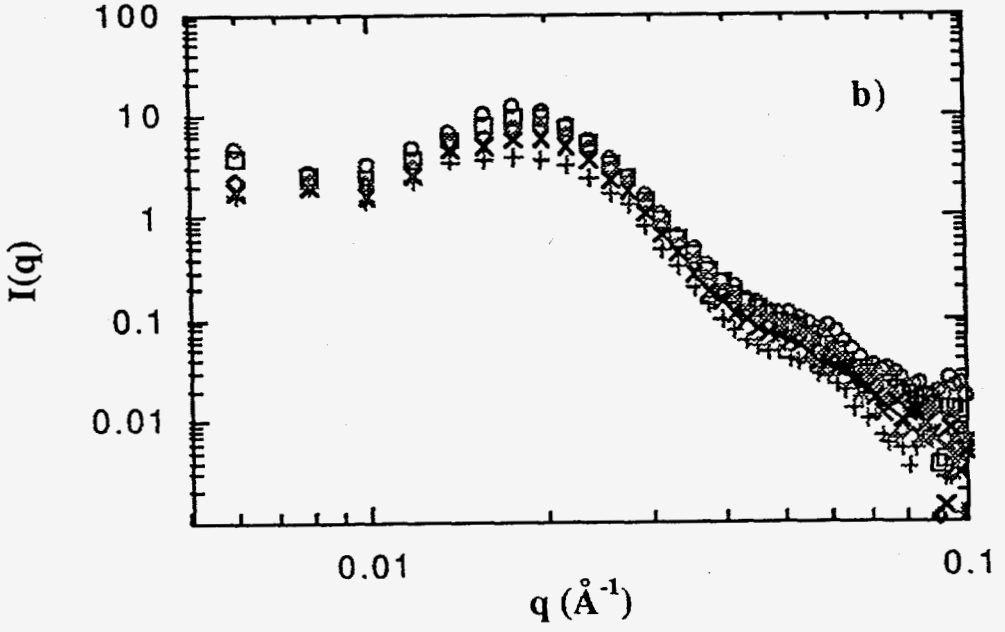
b)
100
10
1
0.1
0.01
I(q)
0.01
0.1
q (Å-1)

a)

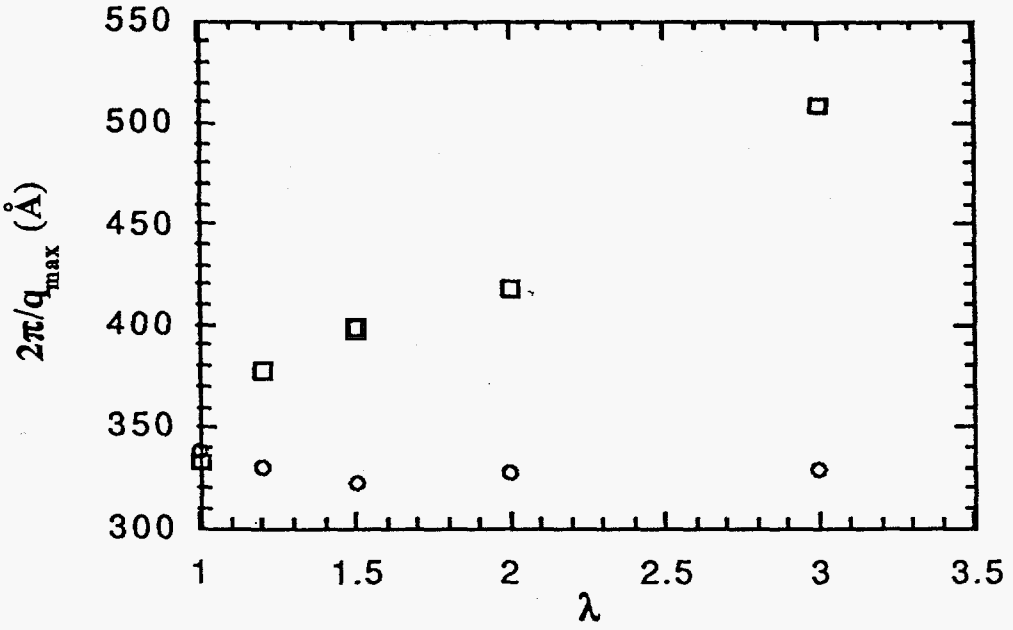
550
500
450
400
350
300
$2\pi/q_{max}$ (Å)
1
1.5
2
2.5
3
3.5
λ

b)

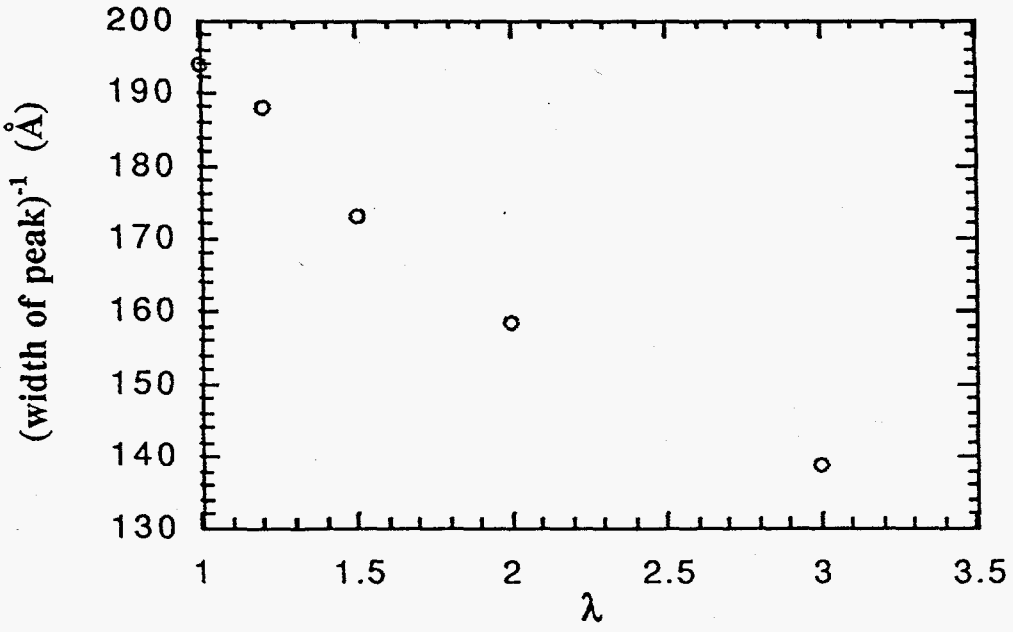
200
190
180
170
160
150
140
130
(width of peak)$^{-1}$ (Å)
1
1.5
2
2.5
3
3.5
λ

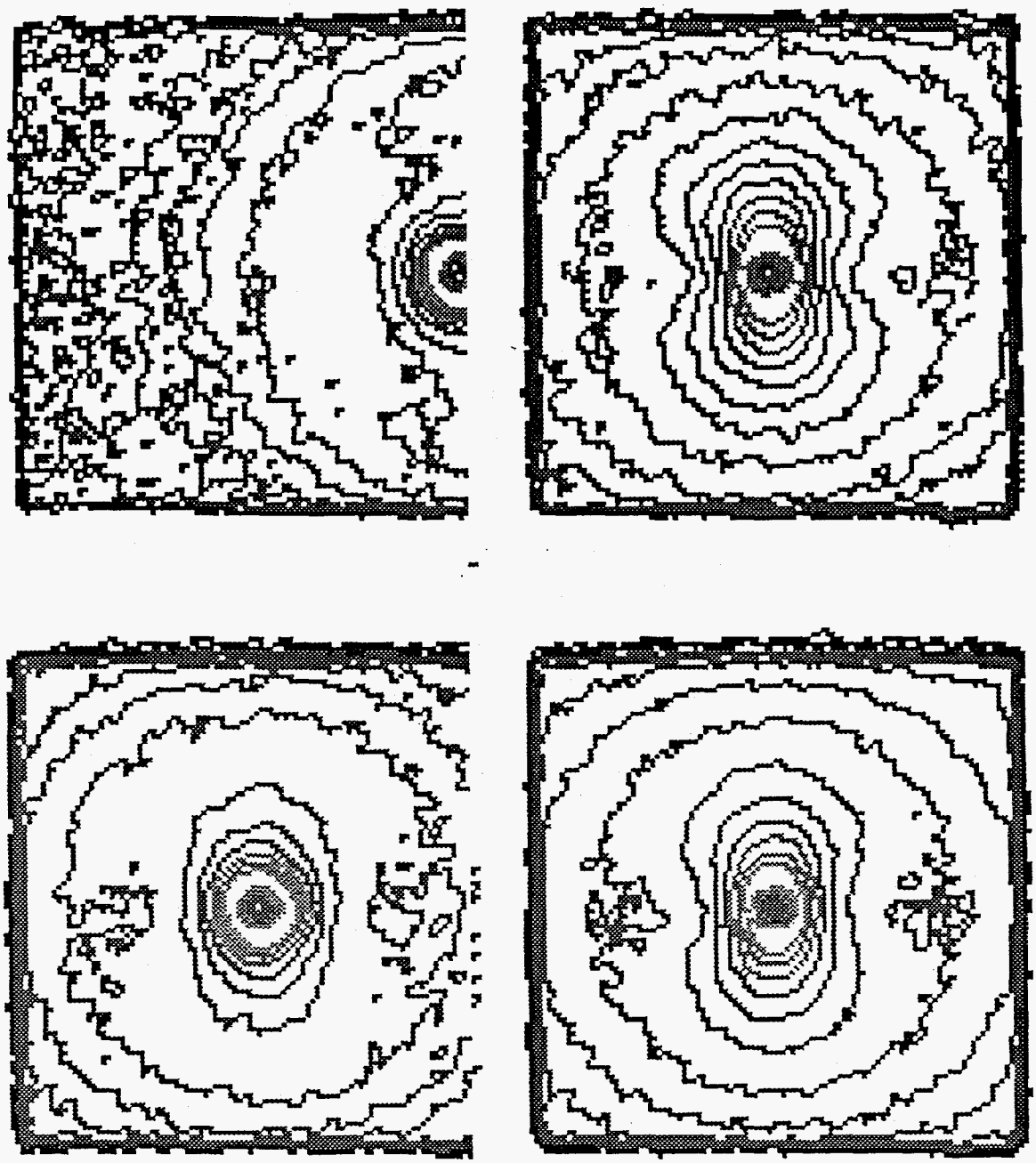

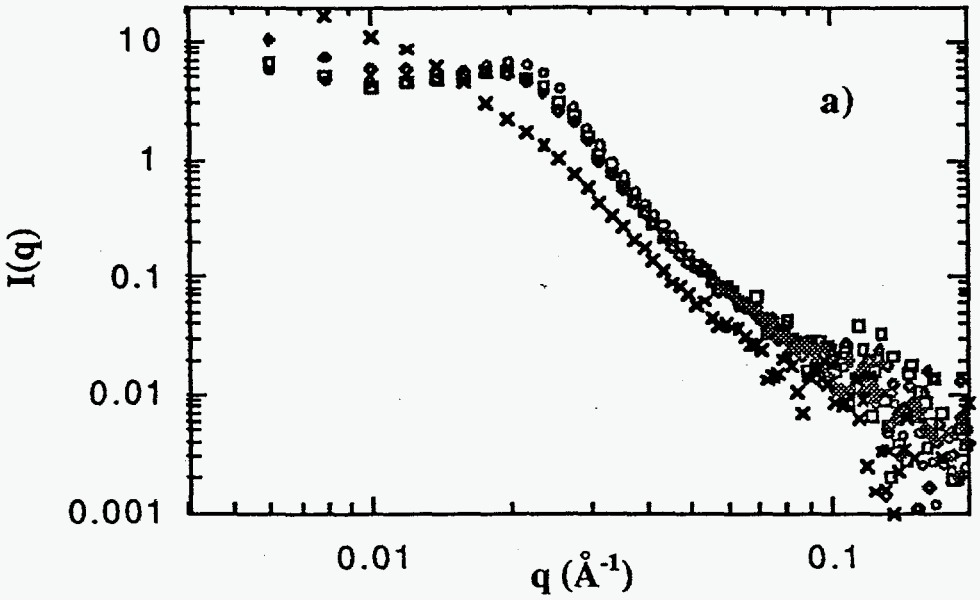
10
1
0.1
0.01
0.001
I(q)
a)
0.01
0.1
q (Å-1)

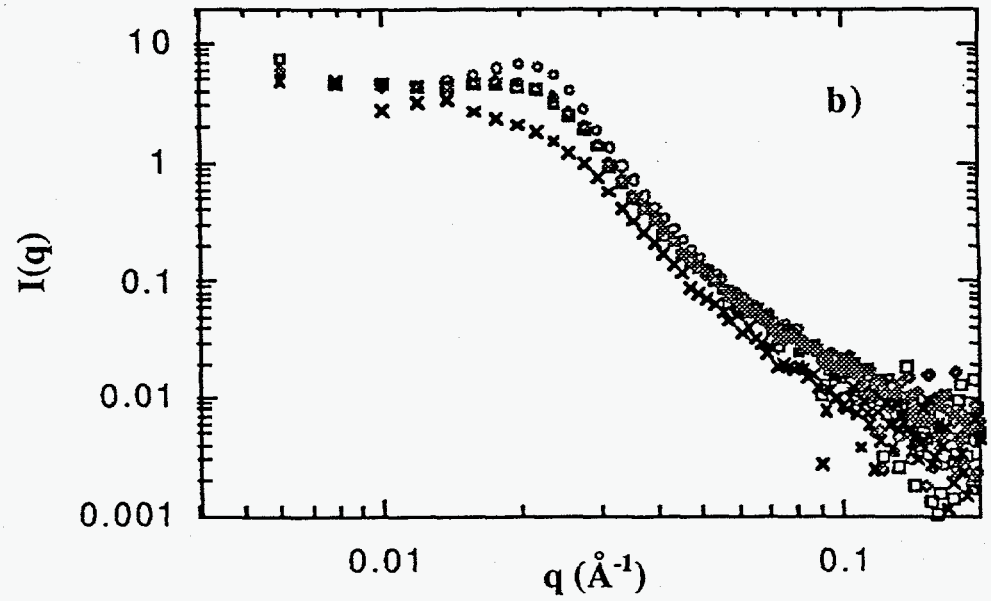
10
1
0.1
0.01
0.001
I(q)
b)
0.01
0.1
q (Å-1)

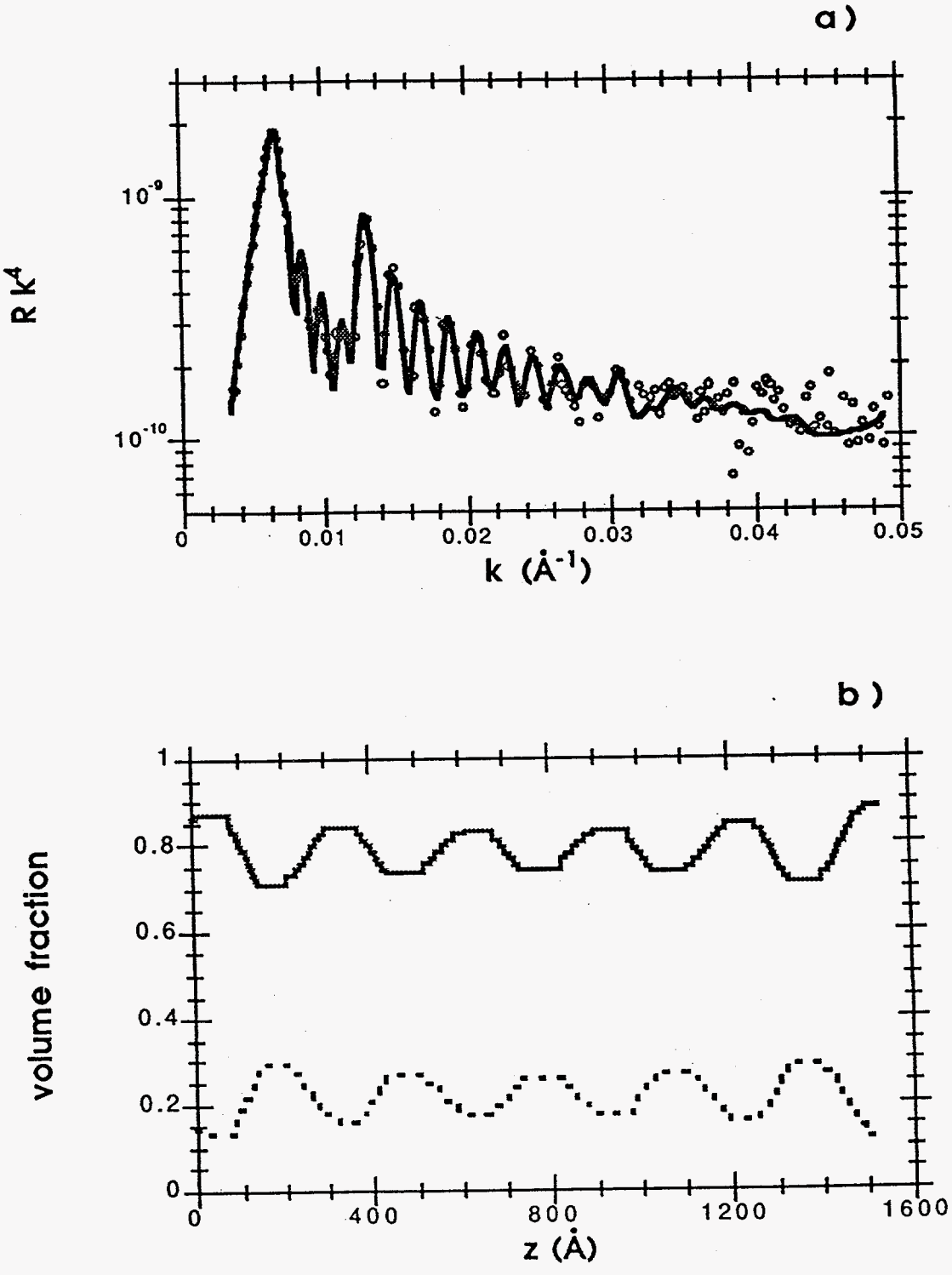
a)
10^{-9}
10^{-10}
R K^4
0
0.01
0.02
0.03
0.04
0.05
k (Å^{-1})
b)
1
0.8
0.6
0.4
0.2
0
volume fraction
0
400
800
1200
1600
z (Å)

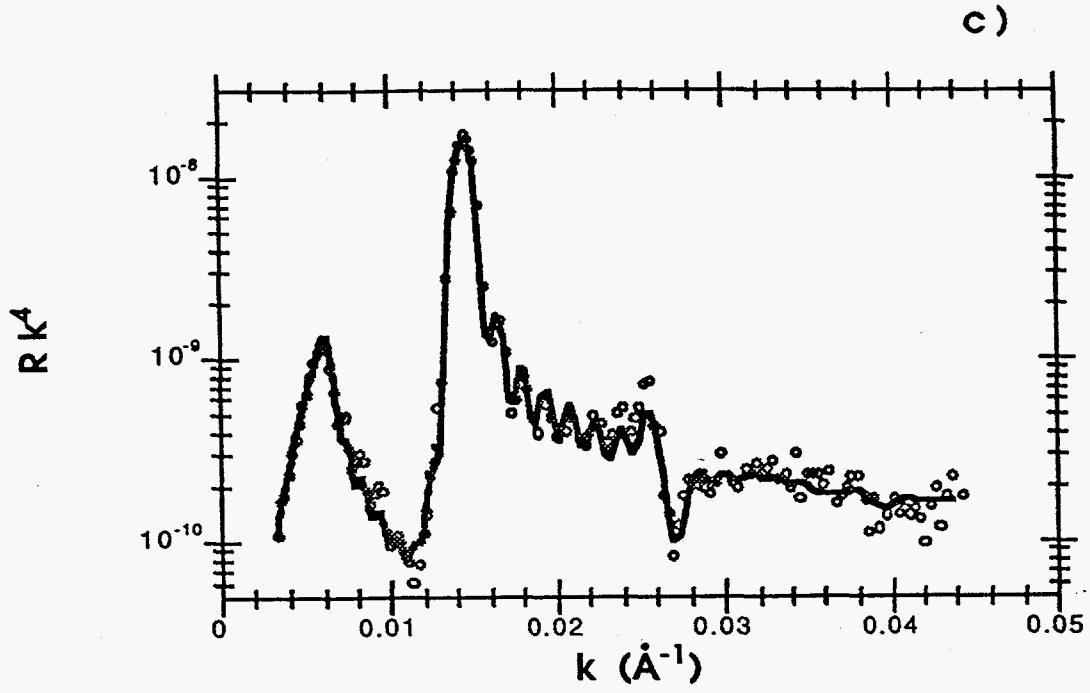
c)
R K⁴
10⁻⁸
10⁻⁹
10⁻¹⁰
0
0.01
0.02
0.03
0.04
0.05
k (Å⁻¹)

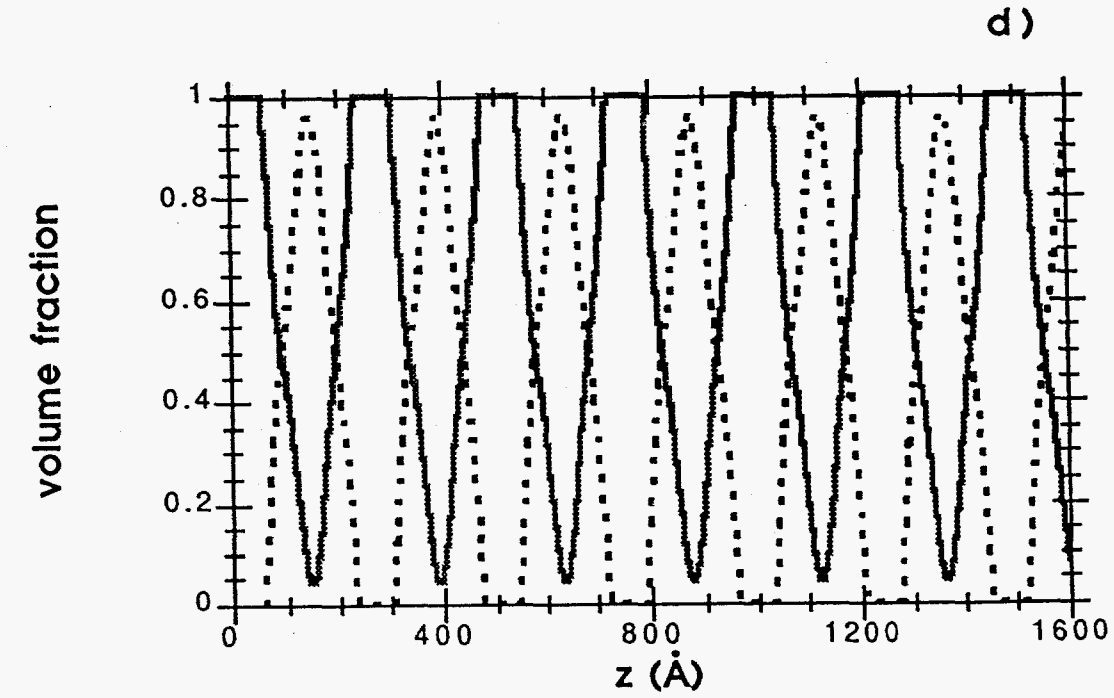
d)
volume fraction
1
0.8
0.6
0.4
0.2
0
0
400
800
1200
1600
z (Å)

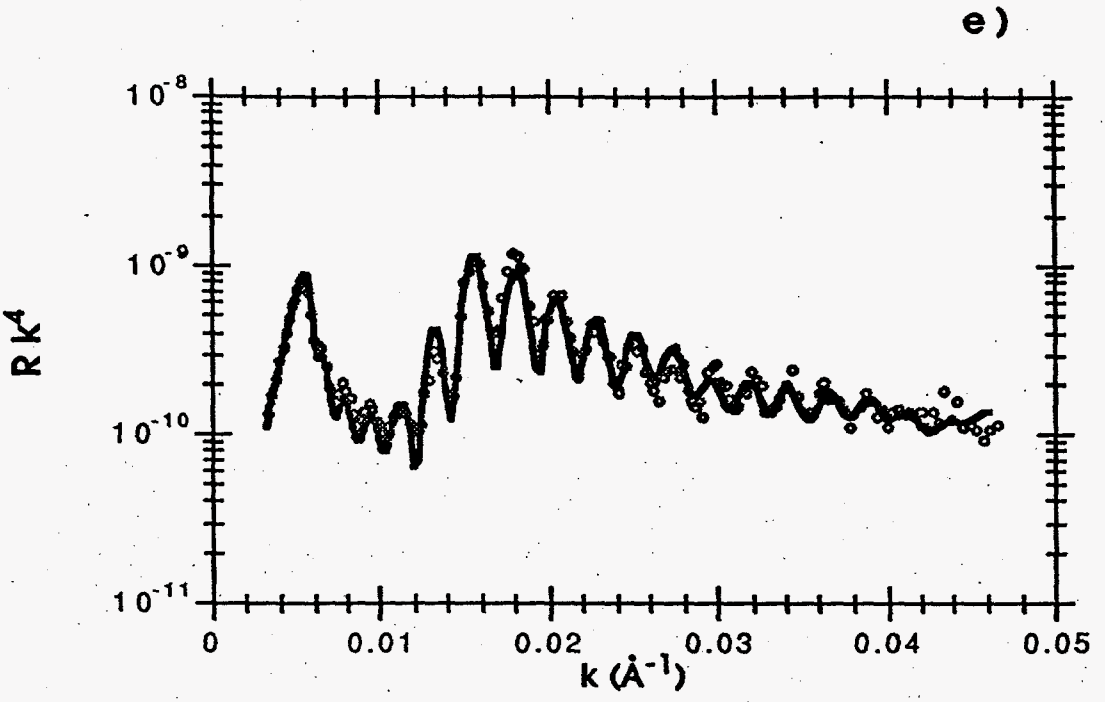
e)
10^{-8}
10^{-9}
10^{-10}
10^{-11}
R K⁴
0
0.01
0.02
0.03
0.04
0.05
k (Å⁻¹)

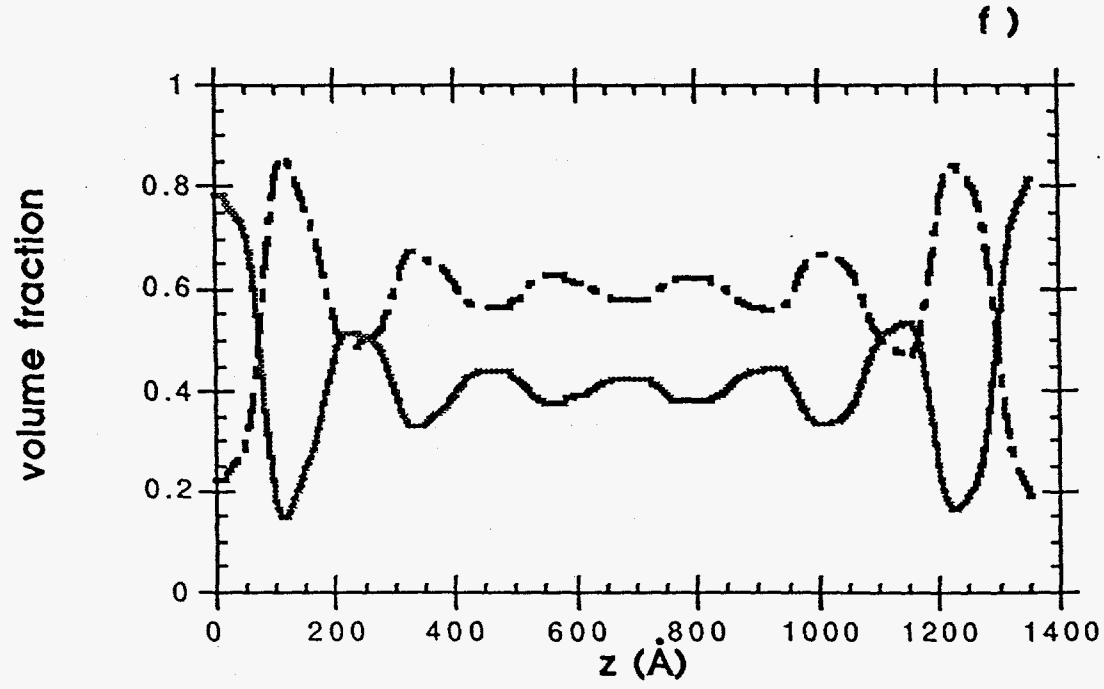
f)
1
0.8
0.6
0.4
0.2
0
volume fraction
0
200
400
600
800
1000
1200
1400
z (Å)

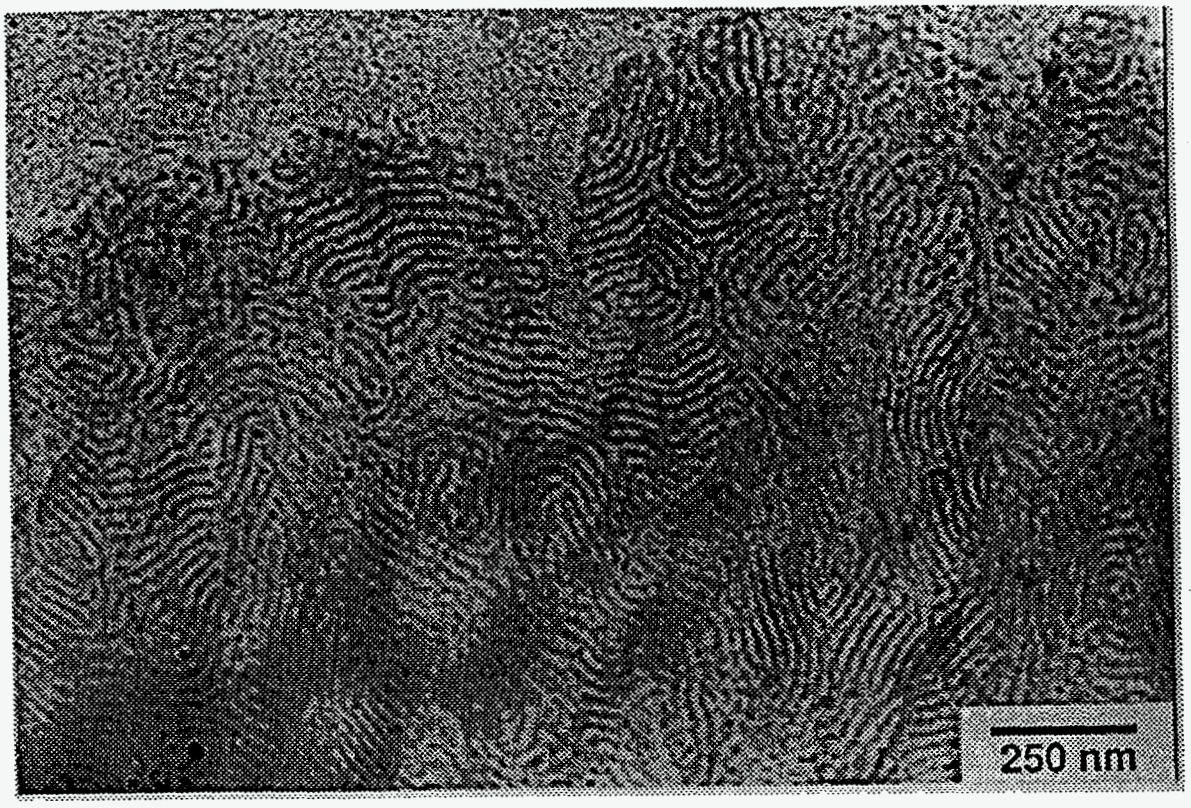
250 nm